JACS
JOURNAL OF THE AMERICAN CHEMICAL SOCIETY

Subscriber access provided by ISTANBUL TEKNIK UNIV

Communication

Self-Propagating Assembly of a Molecular-Based Multilayer

Leila Motiei, Marc Altman, Tarkeshwar Gupta, Fabio Lupo, Antonino Gulino, Guennadi Evmenenko, Pulak Dutta, and Milko E. van der Boom

J. Am. Chem. Soc., **2008**, 130 (28), 8913-8915 • DOI: 10.1021/ja802470g • Publication Date (Web): 24 June 2008

Downloaded from http://pubs.acs.org on February 8, 2009

More About This Article

Additional resources and features associated with this article are available within the HTML version:

- Supporting Information
- Access to high resolution figures
- Links to articles and content related to this article
- Copyright permission to reproduce figures and/or text from this article

View the Full Text HTML

ACS Publications
High quality. High impact.

Journal of the American Chemical Society is published by the American Chemical Society. 1155 Sixteenth Street N.W., Washington, DC 20036

J|A|C|S
COMMUNICATIONS

Published on Web 06/24/2008

Self-Propagating Assembly of a Molecular-Based Multilayer

Leila Motiei,[†] Marc Altman,[†] Tarkeshwar Gupta,[†] Fabio Lupo,[‡] Antonino Gulino,[‡] Guennadi Evmenenko,[§] Pulak Dutta,[§] and Milko E. van der Boom*[,†]

Department of Organic Chemistry, Weizmann Institute of Science, Rehovot 76100, Israel, Dipartimento di Scienze Chimiche, Università di Catania, Catania 95125, Italy, and Department of Physics and Astronomy and the Materials Research Center, Northwestern University, Evanston, Illinois 60208-3113

Received April 4, 2008; E-mail: milko.vanderboom@weizmann.ac.il

Chemisorptive layer-by-layer self-assembly (SA) with well-defined molecular components can yield functional organic superlattices on a large variety of substrates,[1–9] which have been used for fabricating nanostructures,[10] light emitting diodes (LEDs),[11] electro-optic modulators,[12] and field-effect transistors (FETs).[13,14] This molecular SA approach can yield highly ordered films whose physicochemical properties (i.e., thickness, optical properties) generally increase linearly with the number of deposition sequences. A rare example of a nonlinear assembly process based on self-replicating amphiphilic monolayers was reported by Sagiv et al.[15] Various polyelectrolyte multilayer films obtained by consecutive adsorption of polyanions and polycations are known to exhibit nonlinear growth.[16–24] The mechanism underlying the formation of this important class of functional materials involves the "inward" and "outward" diffusion of polyelectrolytes throughout the thin polymer layers during the deposition process.[18–25]

Is it possible to generalize the mechanism governing the growth of polyelectrolyte films to other systems? Exponential growth of molecular-based films is highly desirable because it would minimize the number of deposition cycles necessary to reach desired material properties. This diffusion scenario may be applied to a molecular-based SA process as well, resulting in exponential film growth. However, the surface-bound assembly must play an active role during the film growth. The design rules are clear: (I) At least one of the components that comprise the SA multilayer must be able to diffuse into the molecular-based structure, which is formed via a porous network of covalent or noncovalent interactions. (II) Upon exposure of the SA multilayer to the other component, the intercalated species must be able to diffuse toward the new solution/surface interface to allow the formation of a new layer. (III) A barrier must be present that prohibits the loss of the intercalated compound.

We chose to construct a hybrid structure consisting of a robust and structurally well-defined polypyridyl osmium complex (**1**) and a commercially available palladium precursor using an iterative two-step assembly method recently reported by us.[1] The three pyridine-based binding sites of the new complex **1** and the 3D geometry allow the formation of a coordinated-based network with palladium(II). The SA structures were formed from solution on surface-bound template layers, as shown in Schemes 1 and 2. The SA multilayers were formed by iterative immersion of the functionalized substrates in tetrahydrofuran (THF) solutions of bis(benzonitrile)dichloropalladium and complex **1**. The benzonitrile ligands are relatively weakly coordinated to the metal center and can be readily replaced by pyridine-based ligands.[1] The films were thoroughly washed and sonicated with copious amounts of various organic solvents between each deposition step.

Scheme 1. Chemical Structure of Complex **1** and Formation of the Template Layer[a]

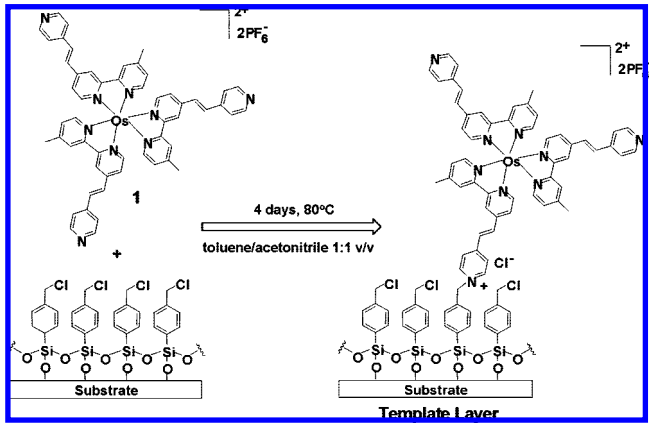

[a] Complex **1**, prepared from $(NH_4)_2OsCl_6$ and 4′-methyl-4-(2-pyridin-4-yl-vinyl)-[2,2′]bipyridyl,[26] was characterized by ^1H and $^{13}C\{^1H\}$ NMR, optical (UV/vis) spectroscopy, elemental (C, H, N) analysis, and mass spectrometry. Chlorobenzyl-functionalized float glass and silicon substrates (0.8 cm × 2.5 cm) were prepared from the corresponding trichlorosilane precursor.[27,28] Subsequently, these substrates were heated in a solution of complex **1** (0.1 mM) under an inert atmosphere of nitrogen. The resulting template layer was washed and sonicated with organic solvents to remove any physisorbed material. The covalently bound films strongly adhere to the substrates and, when stored with the exclusion of light, were stable for months.

UV/vis measurements in the transmission mode of the glass-bound assemblies show the characteristic singlet and triplet metal-to-ligand charge-transfer (MLCT) bands of complex **1** at λ_{max} = 510 and 680 nm, respectively (Figure 1). Remarkably, the intensity of the optical absorption increases exponentially with the number of deposition cycles.

The film thickness derived from two independent methods (XRR and ellipsometry) increases exponentially with the number of deposition cycles, which is in agreement with the optical data (Figure 2A). The same exponential fit is applicable to the optical and structural data. For a microstructurally regular multilayer, the absorption intensity is expected to scale linearly with the increase of the film thickness.[1] Indeed, the observed linear dependence and zero intercept of the absorption at $\lambda = 510$ nm on the XRR-derived thickness demonstrate that approximately equal densities of uniformly oriented chromophores (**1**) are deposited in each deposition cycle while maintaining structural regularity (Figure 2B). In support of this correlation, the XRR-derived electron density $\rho = 0.41$ eÅ^{-3}, for complex **1**-terminated multilayers remained constant throughout the assembly process, indicating the formation of a homogeneous superlattice. The surface of the assembly is relatively smooth. For instance, the XRR measurements indicate a film surface roughness of ∼2 nm for a 35 nm thick structure. In addition, semicontact

[†] Weizmann Institute of Science.
[‡] Università di Catania.
[§] Northwestern University.

 © 2008 American Chemical Society

Scheme 2. Presentation of the Two-Step Solution-Based Assembly Process[a]

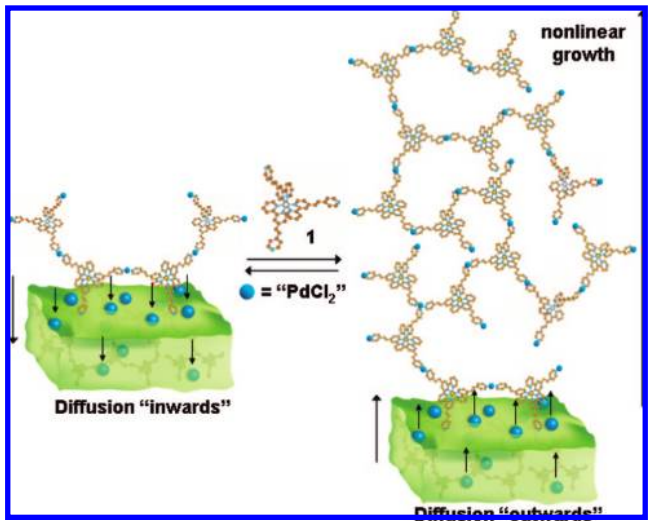

[a] The film growth can be conveniently carried out in air at room temperature using our previously reported method.[1] The SA multilayers were formed by iterative immersion of the functionalized substrates in THF solutions of bis(benzonitrile)dichloropalladium, $(PhCN)_2PdCl_2$ (1 mM), and complex **1** (0.2 mM). The solution of complex **1** contains dimethylformamide (DMF; 10% v/v) to solubilize this compound. The solutions were reused. Discarding solutions to avoid cross-contamination afforded similar results.

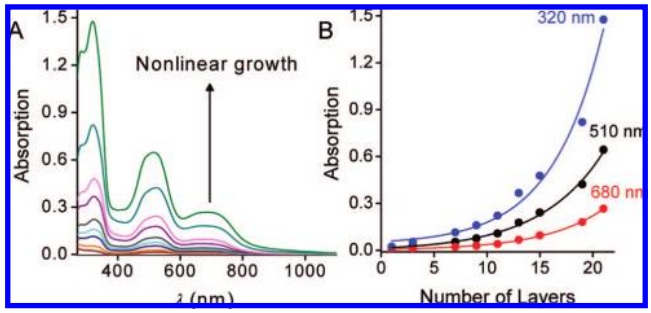

Figure 1. (A) Representative transmission optical absorbance spectra of the multilayers terminated with layers of complex **1**. (B) Exponential dependence of the intensities of the absorption band at $\lambda = 320$ nm and the metal-to-ligand charge-transfer (MLCT) bands at $\lambda = 510$ nm and $\lambda = 680$ nm versus the number of layers ($R^2 > 0.984$ for the exponential fits).

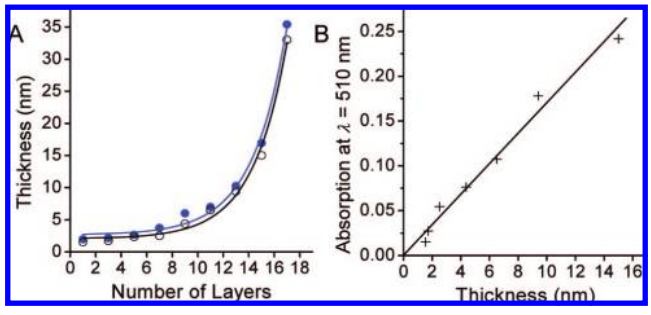

Figure 2. (A) Exponential dependence of the multilayer thickness in nanometers versus the number of layers; ellipsometry (●) and XRR (○) with $R^2 > 0.986$ for the exponential fits. (B) Linear dependence with the XRR-derived thickness as a function of the optical absorption at $\lambda = 510$ nm ($R^2 = 0.981$).

AFM analysis revealed the formation of a continuous interface without pinholes or cracks. The aqueous static contact angle, $\theta_a \approx 65°$, remained constant during the multilayer buildup.

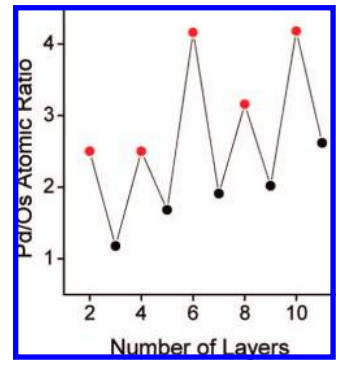

Figure 3. XPS analysis of the palladium and osmium atomic concentrations. Atomic ratio of palladium/osmium versus the number of layers. Even-numbered layers have been exposed to a solution of the palladium precursor (red), whereas odd-numbered layers have been exposed to complex **1** (black). The line serves to guide the eye.

XPS studies provide the elemental composition of the assemblies that confirm the diffusion-controlled growth. The Os/N ratio is within the range 1:8.1−10.5, which is in agreement with the expected ratio of 1:9, demonstrating that there is no significant amount of benzonitrile ligand of the palladium precursor integrated in the film structure. Importantly, the amount of palladium(II) roughly increases by a factor of 2 when the multilayer is exposed to a solution of the palladium precursor (Figure 3), implying intercalation of this component into the film structure. Angle-resolved XPS measurements of an eight-layered assembly revealed that the Pd/Os atomic concentration ratio is the same for different takeoff angles, indicating that the distribution of the excess palladium is uniform, as expected for a porous film structure. For a fully formed network in which all the pyridine moieties of complex **1** are bridged by palladium centers, the expected Pd/Os ratio would be 1.5:1. The overall Pd/Os atomic concentration ratio increases by about a factor of 2, from 1.2 to 2.6 during the formation of an 11-layered structure, suggesting that not all the trapped palladium is being used by the system to build up layers with complex **1**. Exposure of the films to a THF solution of complex **1** significantly decreases the Pd/Os ratio, whereas the total amount of palladium does not decrease. This indicates that the palladium does not diffuse out of the multilayer structure into either the solution of complex **1** or into organic solvents used for washing and sonication. Apparently, there is some barrier that prevents loss of this essential component. The lack of a suitable ligand (e.g., benzonitrile) may contribute to this phenomenon. Similar diffusion-related phenomena have been observed for polyelectrolyte systems.[18–24] The excess of palladium stored in the molecular-based assembly is used by the system to generate another terminal hybrid layer, while retaining the structural organization.

The exponential growth observed with our molecular-based multilayer can be described by considering the assembly in terms of a simple mathematical model. Assuming that the amount of complex **1** deposited in each nominal "layer" (i.e., deposition cycle) is directly proportional to the quantity of palladium dichloride stored in the underlying film, we obtain the following equation:

$$C(n) = \sum_{i=2}^{(n+1)2} [B_{(n-3)2,i-2} + B_{(n-1)2,i-2}b] \cdot a^{i-2} \qquad (1)$$

where $C(n)$ is the number of chromophores deposited in layer n, $B_{m,k}$ is the coefficient of binomial expansion: $m!/(k!(m-k)!)$. The efficiency of the palladium coordination and the storage efficiency of the film for the palladium precursor are expressed as a and b,

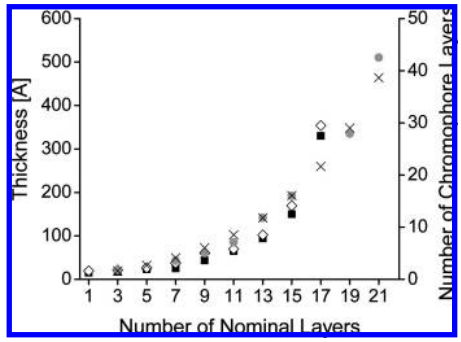

Figure 4. Comparision of exponential growth model (×) with normalized UV/vis absorption (gray dot) (right axis), XRR (■), and ellipsometrically (◇) determined thickness (left axis).

respectively. Summing $C(n)$ over all layers converges to the exponential growth observed. This is consistent with the derivation of the exponential growth in polyelectrolyte films reported by Schaaf and co-workers.[20–22,24] With the constants set empirically at $a = 0.31$ and $b = 0.6$, eq 1 effectively describes the exponential growth of the molecular-based film, as observed by XRR, ellipsometry, and UV/vis absorption (Figure 4). Experimentally, the number of chromophore layers was approximated by normalizing the UV/vis absorption by the absorption of a film containing a single layer of chromophore **1**.

Accelerated growth of a molecular-based material that is an active participant in its continuing self-propagated assembly is demonstrated. This may have implications for the formation of all-organic devices and structures where a large number of deposition steps are generally required to form high-quality, functional materials.[2,7,10–14,29,30] We have recently shown that the layer-by-layer assembly of palladium dichloride and rigid-rod chromophores containing two terminal pyridine moieties resulted in "regular" linear growth of the multilayer versus the number of deposition cycles.[1] The molecular structure of the components and the resulting multilayer properties are key to the nonlinear growth process. The here presented solid-state assembly is actively involved in the growth process rather than acting like a template layer as is usually the case. Apparently, the 3D geometry of complex **1** affords a porous film structure which includes active sites conducive to storage of palladium. One could conjecture that palladium species may bind to the carbon−carbon double bonds of complex **1**, although we do not observe it by UV/vis spectroscopy. Alternatively, the metal-organic network itself may be dynamic, rather than rigid, in nature, and exposure to the palladium-based solution might result in the formation of some monopyridyl−palladium complexes. The *trans*-pyridine−palladium bond is probably weak (~33 kcal/mol) and prone to dissociation.[31] While we cannot discount this scenario, it appears unlikely since the integrity of the films is not compromised at any time during the assembly process. Furthermore, UV/vis measurements show that our films do not disintegrate when treated in THF/DMF (9:1 v/v) at elevated temperatures (45 °C) for 3 h, even in the presence of excess of complex **1** (1.0 mM). The postulated diffusion-controlled mechanism underlying the self-assembly process is in agreement with the experimental and theoretical observations for the exponential growth of certain polyelectrolyte films.[18–25] We have shown that the important characteristics of polyelectrolyte-based films and the here introduced molecular SA system are analogous, suggesting that the rich chemistry of surfaces engineered with molecular-based multilayers may be extended to some of the important functions of polyelectrolyte-based films.[18,32–34]

Acknowledgment. This research was supported by the Helen and Martin Kimmelman Center for Molecular Design and NATO (SfP 981964). T.G. thanks the EU for a Marie Curie fellowship. M.E.vd.B. is the incumbent of the Dewey David Stone and Harry Levine Career Development Chair and Head of a Minerva Junior Research Group. A.G. thanks the Ministero Istruzione Università e Ricerca (MUR, Roma, PRIN 2005 and FIRB 2003). XRR measurements were performed at the National Synchrotron Light Source on Beamline X-23B, which is supported by the Naval Research Laboratory. G.E. and P.D. were supported by the U.S. Department of Energy under Grant DE-FG02-84ER45125.

Supporting Information Available: Formation and characterization data for complex **1** and details of the assembly process. This material is available free of charge via the Internet at http://pubs.acs.org.

References

(1) (a) Altman, M.; Zenkina, O.; Evmenenko, G.; Dutta, P.; van der Boom, M. E. *J. Am. Chem. Soc.* **2008**, *130*, 5040–5041. (b) Altman, M.; Shukla, A. D.; Zubkov, T.; Evmenenko, G.; Dutta, P.; van der Boom, M. E. *J. Am. Chem. Soc.* **2006**, *128*, 7374–7382.
(2) (a) Onclin, S.; Ravoo, B. J.; Reinhoudt, D. N. *Angew. Chem., Int. Ed.* **2005**, *44*, 6282–6304. (b) Mallouk, T. E.; Gavin, J. A. *Acc. Chem. Res.* **1998**, *31*, 209–217. (c) Yitzchaik, S.; Marks, T. J. *Acc. Chem. Res.* **1996**, *29*, 197–202. (d) Ulman, A. *An Introduction to Ultrathin Organic Films: From Langmuir−Blodgett to Self-Assembly*; Academic: San Diego, 1991.
(3) Wanunu, M.; Vaskevich, A.; Cohen, S. R.; Cohen, H.; Arad-Yellin, R.; Shanzer, A.; Rubinstein, I. *J. Am. Chem. Soc.* **2005**, *127*, 17877–17887.
(4) Flory, W. C.; Mehrens, S. M.; Blanchard, G. J. *J. Am. Chem. Soc.* **2000**, *122*, 7976–7985.
(5) Katz, H. E.; Scheller, G.; Putvinski, T. M.; Schilling, M. L.; Wilson, W. L.; Chidsey, C. E. D. *Science* **1991**, *254*, 1485–1487.
(6) Lee, H.; Kepley, L. J.; Hong, H.-G.; Mallouk, T. E. *J. Am. Chem. Soc.* **1988**, *110*, 618–620.
(7) Li, D. Q.; Ratner, M. A.; Marks, T. J.; Zhang, C.; Yang, J.; Wong, G. K. *J. Am. Chem. Soc.* **1990**, *112*, 7389–7390.
(8) Netzer, L.; Sagiv, J. *J. Am. Chem. Soc.* **1983**, *105*, 674–676.
(9) Cao, G.; Hong, H.-G.; Mallouk, T. E. *Acc. Chem. Res.* **1992**, *25*, 420–427.
(10) Hatzor, A.; Weiss, P. S. *Science* **2001**, *291*, 1019–1020.
(11) Burtman, V.; Zelichenok, A.; Yitzchaik, S. *Angew. Chem., Int. Ed.* **1999**, *38*, 2041–2045.
(12) Facchetti, A.; Annoni, E.; Beverina, L.; Morone, M.; Zhu, P.; Marks, T. J.; Pagani, G. A. *Nat. Mater.* **2004**, *3*, 910–917.
(13) Wang, L.; Yoon, M.-H.; Lu, G.; Yang, Y.; Facchetti, A.; Marks, T. J. *Nat. Mater.* **2006**, *5*, 893–900.
(14) Yoon, M.-H.; Facchetti, A.; Marks, T. J. *Proc. Natl. Acad. Sci. U.S.A.* **2005**, *102*, 4678–4682.
(15) Maoz, R.; Matlis, S.; DiMasi, E.; Ocko, B. M.; Sagiv, J. *Nature* **1996**, *384*, 150–153.
(16) DeLongchamp, D. M.; Kastantin, M.; Hammond, P. T. *Chem. Mater.* **2003**, *15*, 1575–1586.
(17) Ji, J.; Fu, J.; Shen, J. *Adv. Mater.* **2006**, *18*, 1441–1444.
(18) Decher, G., Schlenoff, J. B., Eds. *Multilayer Thin Films*; Wiley-VCH: Weinheim, Germany, 2003.
(19) Kujawa, P.; Moraille, P.; Sanchez, J.; Badia, A.; Winnik, F. M. *J. Am. Chem. Soc.* **2005**, *127*, 9224–9234.
(20) Lavalle, P.; Picart, C.; Mutterer, J.; Gergely, C.; Reiss, H.; Voegel, J.-C.; Senger, B.; Schaaf, P. *J. Phys. Chem. B* **2004**, *108*, 635–648.
(21) Picart, C.; Mutterer, J.; Richert, L.; Luo, Y.; Prestwich, G. D.; Schaaf, P.; Voegel, J.-C.; Lavalle, P. *Proc. Natl. Acad. Sci. U.S.A.* **2002**, *99*, 12531–12535.
(22) Porcel, C.; Lavalle, P.; G; Decher, G.; Senger, B.; Voegel, J.-C.; Schaaf, P *Langmuir* **2007**, *23*, 1898–1904.
(23) Wood, K. C.; Chuang, H. F.; Batten, R. D.; Lynn, D. M.; Hammond, P. T. *Proc. Natl. Acad. Sci. U.S.A.* **2006**, *103*, 10207–10212.
(24) Porcel, C.; Lavalle, P.; Ball, V.; Decher, G.; Senger, B.; Voegel, J.-C.; Schaaf, P. *Langmuir* **2006**, *22*, 4376–4383.
(25) Salomaki, M.; Vinokurov, I. A.; Kankare, J. *Langmuir* **2005**, *21*, 11232–11240.
(26) Williams, J. L. R.; Adel, R. E.; Carlson, J. M.; Reynolds, G. A.; Borden, D. G.; Ford, J. A., Jr *J. Org. Chem.* **1963**, *28*, 387–390.
(27) Yerushalmi, R.; Scherz, A.; van der Boom, M. E. *J. Am. Chem. Soc.* **2004**, *126*, 2700–2701.
(28) Li, D. Q.; Swanson, B. I.; Robinson, J. M.; Hoffbauer, M. A. *J. Am. Chem. Soc.* **1993**, *115*, 6975–6980.
(29) Zhang, X.; Chen, H.; Zhang, H. *Chem. Commun.* **2007**, 1395–1405.
(30) Ariga, K.; Hill, J. P.; Ji, Q. *Phys. Chem. Chem. Phys.* **2007**, *9*, 2319–2340.
(31) Ray, L.; Shaikh, M. M.; Ghosh, P. *Dalton Trans.* **2007**, 4546–4555.
(32) Esker, A. R.; Mengel, C.; Wegner, G. *Science* **1998**, *280*, 892.
(33) Benkirane-Jessel, N.; Lavalle, P.; Ball, V.; Ogier, J.; Senger, B.; Picart, C.; Schaaf, P.; Voegel, J.-C.; Decher, G. *Macromol. Eng.* **2007**, *2*, 1249–1305.
(34) Decher, G. *Science* **1997**, *277*, 1232–1237.

JA802470G